A rearrangement minimization problem corresponding to p -Laplacian equation

Kao, Chiu-Yen; Mohammadi, S.A.

Published in:
ESAIM: Control, Optimisation and Calculus of Variations

DOI:
10.1051/cocv/2022004

Publication date:
2022

ESAIM: COCV 28 (2022) 11
https://doi.org/10.1051/cocv/2022004

ESAIM: Control, Optimisation and Calculus of Variations
www.esaim-cocv.org

A REARRANGEMENT MINIMIZATION PROBLEM CORRESPONDING TO p-LAPLACIAN EQUATION

Chiu-Yen Kao[1,*] and Seyyed Abbas Mohammadi[2,**]

Abstract. In this paper a rearrangement minimization problem corresponding to solutions of the p-Laplacian equation is considered. The solution of the minimization problem determines the optimal way of exerting external forces on a membrane in order to have a minimum displacement. Geometrical and topological properties of the optimizer is derived and the analytical solution of the problem is obtained for circular and annular membranes. Then, we find nearly optimal solutions which are shown to be good approximations to the minimizer for specific ranges of the parameter values in the optimization problem. A robust and efficient numerical algorithm is developed based upon rearrangement techniques to derive the solution of the minimization problem for domains with different geometries in $\mathbb{R}^2$ and $\mathbb{R}^3$.

Mathematics Subject Classification. 35Q93, 49J20, 49M99, 35J20, 74E30.

Received August 5, 2021. Accepted January 17, 2022.

1. Introduction

Rearrangement (shape) optimization problems arise in many different fields of applications such as fluid and structural mechanics, population biology, photonic crystals and nano structures, see [1, 4, 5, 9–12, 14, 24–26, 30, 31, 36, 40, 42–44], to name just a few. In such problems, a functional corresponding to solutions of a given differential equation should be optimized over a rearrangement class of functions. In most applications, the rearrangement class is in one to one correspondence of a set of domains with different shapes and so one can recast the optimization problem as an optimal shape design problem.

In this paper, we consider a rearrangement minimization problem corresponding to solutions of the Poisson equation of p-Laplacian. Let Ω be a bounded domain in $\mathbb{R}^N$ with smooth boundary and $f(\mathbf{x}) \in L^\infty(\Omega)$ be a non-negative function. We consider the following boundary value problem

$$-\Delta_p u = f(\mathbf{x}) \text{ in } \Omega, \quad u(\mathbf{x}) = 0 \text{ on } \partial\Omega, \tag{1.1}$$

where $\Delta_p := \operatorname{div}(|\nabla u|^{p-2}\nabla u)$ is the $p-$Laplacian operator with $p \in (1, +\infty)$.

*This author's work is supported in part by a NSF grant DMS-1818948.

Keywords and phrases: p-Laplacian; rearrangement minimization; analytical solution; rearrangement algorithms; membranes.

[1] Department of Mathematical Sciences, Claremont McKenna College, Claremont, CA 91711, USA.
[2] Department of Mathematics, College of Sciences, Yasouj University, Yasouj, 75918-74934, Iran.

** Corresponding author: mohammadi@yu.ac.ir

We say a function $u \in W_0^{1,p}(\Omega)$ is a solution of (1.1) if it satisfies

$$\int_\Omega |\nabla u|^{p-2}\nabla u \cdot \nabla\phi \mathrm{d}\mathbf{x} = \int_\Omega f\phi \mathrm{d}\mathbf{x}, \quad \text{for all} \quad \phi \in W_0^{1,p}(\Omega). \tag{1.2}$$

In order to emphasize the dependence of the solution on f, we denote the solution by u_f. It is well-known that (1.1) has a unique solution and $u_f > 0$ in Ω due to the strong maximum principle when $f \not\equiv 0$ [7, 21, 51].

Defining the functional $\mathcal{F}(f) = \int_\Omega f u_f \mathrm{d}\mathbf{x}$ we will study the minimization problem

$$\min_{f\in\mathcal{M}} \mathcal{F}(f), \tag{1.3}$$

where $\mathcal{M} = \left\{f \in L^\infty(\Omega) : \ \alpha \le f(\mathbf{x}) \le \beta, \ \int_\Omega f(\mathbf{x})\mathrm{d}\mathbf{x} = \gamma\right\}$ such that $\beta > \alpha \ge 0$ and $\gamma > 0$.

It is established that problem (1.3) has a bang-bang optimizer *i.e.*, there is a solution of the form $\hat{f}(\mathbf{x}) = \alpha + (\beta-\alpha)\chi_{\hat{D}}(\mathbf{x})$ such that $|\hat{D}| = A$ where $A = \frac{\gamma-\alpha|\Omega|}{(\beta-\alpha)}$. This reveals that we can recast (1.3) as an optimization problem over the set $\mathcal{N} = \{f : \ f = \alpha + (\beta-\alpha)\chi_D, \ |D| = A\}$ which is a rearrangement class of functions, see Section 2 for the definition and a summary of properties concerning rearrangements. Indeed (1.3) is a shape optimization problem where we are searching for an optimal set or optimal shape design $\hat{D} \subset \Omega$ with $|\hat{D}| = A$ which minimizes the functional $\mathcal{F} = \mathcal{F}(D)$.

Let us describe the physical importance of (1.3) which is most realistic when $p = 2$. In mechanical vibration, (1.1) models the steady state of a vibrating membrane of a prescribed shape $\Omega \subset \mathbb{R}^2$ with a vertical force $f(\mathbf{x})$, *e.g.* gravity and external loads, applied to it. Furthermore, let the membrane be perfectly flexible and elastic which means that the magnitude of the tension is constant. Then, $u_f(\mathbf{x})$ is the deformation of the membrane from the rest position and $\mathcal{F}(f)$ is the total displacement of it which in a way measures the robustness for the membrane [36, 47]. Given a total amount of energy $\int_\Omega f(\mathbf{x})\mathrm{d}\mathbf{x} = \gamma$, we want to minimize $\mathcal{F}(f)$ by exerting a force $f(\mathbf{x})$ where $m \le f(\mathbf{x}) \le M$. Indeed, here we are tuning the force in a way that leads to a smaller displacement. For non ideal materials, *e.g.* power-low solids, it is often appropriate to involve a power of the gradient $|\nabla u|$ to describe the law governing the model. The solution of equation (1.1) for $p \neq 2$, can be considered as a model for membranes made out of such non ideal materials [2, 16]. As another application, equation (1.1) can be considered as a stationary heat transfer equation for a body $\Omega \subset \mathbb{R}^3$ where $u(\mathbf{x})$ is the temperature of the body at point $\mathbf{x}$. Actually in (1.1) the heat flux is a nonlinear function of the temperature gradient [49]. The body is surrounded by a region *e.g.*, air, with zero temperature. The external source $f(\mathbf{x})$ supplies heat and $\int_\Omega f(\mathbf{x})\mathrm{d}\mathbf{x} = \gamma$ is the total amount of heat energy which is available by the source. Let $\alpha = 0$, the optimal set $\hat{D}$ is a region in the body that should be heated to minimize $\mathcal{F}(D)$ which in this case, up to a normalization constant, the amount of heat presented in the region occupied by D [17, 47]. It is noteworthy that equation (1.1) and the corresponding optimization problem (1.3) can be interpreted differently, for instance see [27, 41].

Optimization problem (1.3) corresponding to nonlinear differential equation (1.1) has been studied by several authors, see [18, 19, 38]. They have addressed existence and uniqueness of solutions of (1.3) using continuity, differentiability and convexity of the functional $\mathcal{F}$. Moreover, the analytical solution has been obtained for the specific case that Ω is a ball invoking symmetrization techniques. However, it is necessary from both mathematical and physical points of view to find solutions of minimization problem (1.3) in general. The problem of obtaining an analytical solution for rearrangement (shape) optimization problems are quite hard since we do not know the topology or geometry of the optimal domain a priori.

To do so, at first in this paper we investigate geometrical and topological properties of the optimal set $\hat{D}$ such as connectivity and symmetry. Employing these properties we derive the analytical solution for the case that Ω is an annulus. Then, we will find nearly optimal solutions which will be established that are in good agreement with the solution of (1.3) for specific ranges of the parameter values in the minimization problem. These nearly optimal solutions can be derived explicitly for several domains. At last, we will develop a robust and efficient numerical algorithm which is capable to determine the solution of (1.3) for different domains in $\mathbb{R}^2$ and $\mathbb{R}^3$.

2. Preliminaries

In this section we will provide results that are needed for our analysis.

As a consequence of the strong maximum principle and Sobolev embedding theorems, we have

$$0 < u_f(\mathbf{x}) \leq C\|f\|_{L^\infty(\Omega)}^{\frac{1}{p-1}}, \tag{2.1}$$

where C depends on p, N and Ω, [7, 21, 51]. Then, from the standard regularity theory, we infer $u_f \in C^{1,r}(\bar{\Omega})$ for some $r \in (0,1)$, [35, 50]. It is noteworthy that u_f is the unique minimizer of the following minimization problem

$$\min_{u \in W_0^{1,p}(\Omega)} \mathcal{G}(u), \tag{2.2}$$

where $\mathcal{G}(u) = \int_\Omega |\nabla u|^p \mathrm{d}\mathbf{x} - p\int_\Omega f u \mathrm{d}\mathbf{x}$ and the minimum value is $(1-p)\mathcal{F}(f) = (1-p)\int_\Omega f u_f \mathrm{d}\mathbf{x}$. Setting $q = \frac{p}{p-1}$ the conjugate exponent of p, the following lemma indicates weak continuity, continuously differentiability and convexity of the functional $\mathcal{F}$ [19, 38].

Lemma 2.1. *a) Consider functions $\{f_n\}_1^\infty$ such that $f_n \rightharpoonup f$ in $L^q(\Omega)$. Then, we have $\mathcal{F}(f_n) \to \mathcal{F}(f)$.*
b) The functional $\mathcal{F}$ is continuously Gateaux differentiable such that

$$(\mathcal{F}'(f), g) = q\int_\Omega g u_f \mathrm{d}\mathbf{x}, \quad \textit{and} \quad \mathcal{F}'(f) = q u_f.$$

c) $\mathcal{F}$ is strictly convex.

Using properties of the functional $\mathcal{F}(f)$ in Lemma 2.1 and Theorem 5.3.9 in [3], we obtain the following optimality condition.

Lemma 2.2. *The function $\hat{f}$ is the minimizer of (1.3) if and only if*

$$\int_\Omega \hat{f} u_{\hat{f}} \mathrm{d}\mathbf{x} \leq \int_\Omega f u_{\hat{f}} \mathrm{d}\mathbf{x}, \quad \textit{for all } f \in \mathcal{M}.$$

2.1. Rearrangements

In this subsection we provide some basic and well-known results about rearrangement theory [9, 10].

Two Lebesgue measurable functions $f : \Omega' \subset \mathbb{R}^N \to \mathbb{R}$, $f_0 : \Omega \subset \mathbb{R}^N \to \mathbb{R}$, are said to be rearrangements of each other if

$$|\{\mathbf{x} \in \Omega' : f(\mathbf{x}) \geq c\}| = |\{\mathbf{x} \in \Omega : f_0(\mathbf{x}) \geq c\}| \qquad \forall c \in \mathbb{R}. \tag{2.3}$$

The set of functions which are rearrangement of $f_0 : \Omega \subset \mathbb{R}^N \to \mathbb{R}$ is called the rearrangement class generated by f_0. Considering $f_0 = \alpha + (\beta - \alpha)\chi_{D_0}$ with $|D_0| = A$, it is easy to check that all functions in $\mathcal{N}$ are rearrangements of f_0 and indeed this set is the rearrangement class generated by f_0. It is well-known that the weak closure of the rearrangement set $\mathcal{N}$ in $L^2(\Omega)$ is the set $\mathcal{M}$ where is convex and weakly sequentially compact. Moreover, for all functions $f \in \mathcal{N}$ we have $\|f\|_{L^2(\Omega)} = \|f_0\|_{L^2(\Omega)}$, [9, 10]. The following Lemma is vital in our analysis.

Lemma 2.3. *Let $g \in L^2(\Omega)$. If there is a non-increasing function ζ such that $\zeta(g) \in \mathcal{N}$, then $\zeta(g)$ is the unique minimizer of the linear functional $L(h) = \int_\Omega hg \mathrm{d}\mathbf{x}$ relative to $h \in \mathcal{M}$.*

Proof. The proof is an easy consequence of Lemma 2.4 in [10]. □

The Steiner symmetrization of a given function u is vital in our analysis when we study symmetric domains. In order to introduce these rearrangements, we recall the notion of Steiner symmetrization of sets. Let $\mathcal{H}^k$ be the Hausdorff k-dimensional outer measure on $\mathbb{R}^N$. Let T be a k-dimensional affine subspace of $\mathbb{R}^N$, $0 \le k \le N-1$. The Steiner symmetrization of a set $E \subset \mathbb{R}^N$ with respect to T is the unique set E^* such that for any $\mathbf{x} \in T$, if L is the $(N-k)$-dimensional hyperplane orthogonal to T that contains $\mathbf{x}$, then

$$E^* \cap L = \mathcal{B}(\mathbf{x}, r) \cap L,$$

where $\mathcal{B}(\mathbf{x}, r)$ is a ball centered at $\mathbf{x}$ with radius $0 \le r \le \infty$ such that $\mathcal{H}^{N-k}(\mathcal{B}(\mathbf{x}, r) \cap L) = \mathcal{H}^{N-k}(E \cap L)$.

Assume Ω is Steiner symmetric, *i.e.*, $\Omega = \Omega^*$. The Steiner symmetrization of nonnegative function $u : \Omega \to \mathbb{R}$ with respect to T is the unique function $u^* : \Omega \to \mathbb{R}$ such that for each $c \in \mathbb{R}$, we have

$$\{\mathbf{x} \in \Omega : u^*(\mathbf{x}) > c\} = \{\mathbf{x} \in \Omega : u(\mathbf{x}) > c\}^*.$$

Indeed, we have

$$u^*(\mathbf{x}) = \sup\left\{c \in \mathbb{R} : \mathbf{x} \in \{\mathbf{y} \in \Omega : u(\mathbf{y}) > c\}^*\right\},$$

and u^* is a rearrangement of u [8].

We will need the following well-known results on Steiner symmetrization.

Lemma 2.4. *Let T be a $(N-1)$-dimensional hyperplane in $\mathbb{R}^N$ and Ω be Steiner symmetric with respect to it, i.e., Ω=Ω^*. Consider non-negative function $u : \Omega \to \mathbb{R}$ in $L^2(\Omega)$ and u^* its Steiner symmetrization with respect to T.If $\xi : \mathbb{R} \to \mathbb{R}$ is Borel measurable then $\int_\Omega \xi(u)\mathrm{d}\mathbf{x} = \int_\Omega \xi(u^*)\mathrm{d}\mathbf{x}$.*

We close this section defining a radial function. Consider $f : \Omega \subset \mathbb{R}^N \to \mathbb{R}$. Setting $r = \|\mathbf{x}\|$, we say that this is a radial function if $f(\mathbf{x}) = f(r)$ for all $\mathbf{x} \in \bar{\Omega}$.

3. Analytical results

This section is devoted to our analytical findings about the minimizer of (1.3) and its corresponding solution of (1.1).

3.1. Existence, uniqueness and geometrical properties

Mimicking the proof of Theorem 2.4 in [19], we obtain the following result.

Theorem 3.1. *The minimization problem (1.3) has a unique solution $\hat{f} = \alpha + (\beta - \alpha)\chi_{\hat{D}}$ such that*

$$\hat{D} = \{\mathbf{x} \in \Omega : \; u_{\hat{f}}(\mathbf{x}) < \hat{t}\}, \quad |\hat{D}| = A. \tag{3.1}$$

Then, we can obtain the following monotonicity theorem for the functional $\mathcal{F}$.

Theorem 3.2. *Let $\hat{f}_1(\mathbf{x}) = \alpha + (\beta - \alpha)\chi_{\hat{D}_1}(\mathbf{x})$ be a solution of (1.3) with $|D_1| = A_1$ and $\hat{f}_2(\mathbf{x}) = \alpha + (\beta - \alpha)\chi_{\hat{D}_2}(\mathbf{x})$ be a solution with $|D_2| = A_2$. Assume $A_1 < A_2$, then we have $\mathcal{F}(\hat{f}_1) < \mathcal{F}(\hat{f}_2)$.*

Proof. Consider $D_1, D_2 \subset \Omega$ such that $D_1 \subset D_2$ and $|D_1| = A_1$, $|D_2| = A_2$. Setting $f_1(\mathbf{x}) = \alpha + (\beta - \alpha)\chi_{D_1}(\mathbf{x})$ and $f_2(\mathbf{x}) = \alpha + (\beta - \alpha)\chi_{D_2}(\mathbf{x})$, we have

$$(1-p)\mathcal{F}(f_1) = \min_{u \in W_0^{1,p}(\Omega)} \int_\Omega |\nabla u|^p \mathrm{d}\mathbf{x} - p\int_\Omega f_1 u \mathrm{d}\mathbf{x} = \int_\Omega |\nabla u_{f_1}|^p \mathrm{d}\mathbf{x} - p\int_\Omega f_1 u_{f_1} \mathrm{d}\mathbf{x}$$

$$> \int_\Omega |\nabla u_{f_1}|^p \mathrm{d}\mathbf{x} - p\int_\Omega f_2 u_{f_1} \mathrm{d}\mathbf{x} \geq (1-p)\mathcal{F}(f_2), \tag{3.2}$$

since $f_1(\mathbf{x}) \leq f_2(\mathbf{x})$ almost everywhere in Ω.

Now, suppose D_1 is an arbitrary subset of $\hat{D}_2$ such that $|D_1| = A_1$. In view of (3.2), we have $\mathcal{F}(f_1) < \mathcal{F}(\hat{f}_2)$ and so we obtain $\mathcal{F}(\hat{f}_1) < \mathcal{F}(\hat{f}_2)$. □

In the following theorem, some topological and geometrical properties of the set $\hat{D}$ are investigated.

Theorem 3.3. *Let $\hat{f} = \alpha + (\beta - \alpha)\chi_{\hat{D}}$ be the unique minimizer of (1.3). Then,*
a) $\hat{D}$ contains a tubular neighborhood of the boundary $\partial\Omega$.
b) Every connected component $\mathcal{D}$ of the interior of $\hat{D}$ touches the boundary, i.e. $\bar{\mathcal{D}} \cap \partial\Omega \neq \emptyset$.
c) In particular, if $\Omega \subset \mathbb{R}^2$ is simply connected then $\hat{D}$ is connected.

Proof. a) It is clear in view of (3.1) and the Dirichlet boundary conditions.
b) In order to establish this part we argue by contradiction. Assume there is an open subset $\mathcal{D} \subset \{\mathbf{x} \in \Omega : u_{\hat{f}}(\mathbf{x}) < \hat{t}\}$ such that $\partial\mathcal{D}$ is a subset of the closure of $\hat{D}^c$. This means that $\partial\mathcal{D} \subset \{\mathbf{x} \in \Omega : u_{\hat{f}}(\mathbf{x}) \geq \hat{t}\}$. Therefore, $u_{\hat{f}}(\mathbf{x}) = \hat{t}$ on $\partial\mathcal{D}$. In view of (3.1), $u_{\hat{f}}(\mathbf{x})$ assumes a minimum at some $\mathbf{x}_0 \in \mathcal{D}$. Invoking the strong maximum principle, $u_{\hat{f}}(\mathbf{x})$ is constant within $\mathcal{D}$ and so we should have $\Delta_p u_{\hat{f}}(\mathbf{x}) \equiv 0$ in $\mathcal{D}$ due to Lemma 7.7 in [20] which is a contradiction.
c) This is a straightforward consequence of part (b). □

In the next theorem, we investigate the symmetry properties of the unique optimizer $\hat{f}$.

Theorem 3.4. *Assume Ω is Steiner symmetric with respect to a hyperplane T and $\hat{f} = \alpha + (\beta - \alpha)\chi_{\hat{D}}$ is the minimizer of (1.3). Then, the set $\hat{D}^c$ is Steiner symmetric with respect to the hyperplane T.*

Proof. Consider non-increasing function $\eta(s)$ where $\eta(s) = \beta$ for $s < \hat{t}$ and $\eta(s) = \alpha$ for $s \geq \hat{t}$. In view of Theorem 3.1, $\hat{f} = \eta(u_{\hat{f}})$ is the unique minimizer of (1.3) and then $u_{\hat{f}}$ is a solution of the following boundary value problem

$$-\Delta_p u = \eta(u) \text{ in } \Omega, \quad u(\mathbf{x}) = 0 \text{ on } \partial\Omega. \tag{3.3}$$

Set $\zeta(s) = -\int_0^s \eta(\tau)\mathrm{d}\tau$. Now employing the method in the proof of Theorem 5.3 in [37], one can infer that $u_{\hat{f}}$ is the unique solution of (3.3) and also is the unique minimizer of the following functional

$$\mathcal{L}(u) = \int_\Omega |\nabla u|^p \mathrm{d}\mathbf{x} + p\int_\Omega \zeta(u)\mathrm{d}\mathbf{x}, \quad \text{for} \quad u \in W_0^{1,p}(\Omega).$$

Employing Lemma 2.4 and Pólya's inequlity, see [46], it is inferred that

$$\mathcal{L}(u_{\hat{f}}) = \int_\Omega |\nabla u_{\hat{f}}|^p \mathrm{d}\mathbf{x} + p\int_\Omega \zeta(u_{\hat{f}})\mathrm{d}\mathbf{x} \geq \int_\Omega |\nabla u^*_{\hat{f}}|^p \mathrm{d}\mathbf{x} + p\int_\Omega \zeta(u^*_{\hat{f}})\mathrm{d}\mathbf{x} = \mathcal{L}(u^*_{\hat{f}}),$$

which yields $u_{\hat{f}} = u^*_{\hat{f}}$ due to the minimality of $u_{\hat{f}}$. This means that $u_{\hat{f}}$ is Steiner symmetric with respect to T and so $\hat{D}^c$ is symmetric in view of formula (3.1). □

3.2. Analytical solution

The main challenging aspect of rearrangement (shape) optimization problems is that finding an analytical solution for such problems are quite hard. Usually an explicit formula of the optimizer is available just in case that Ω is a ball and the solution is derived using symmetrization techniques, see for instance [23]. In addition to a ball, we derive the analytical solution of (1.3) when Ω is an annulus.

Theorem 3.5. *Let $\Omega = \mathcal{B}(\mathbf{0}, \bar{r})$ with $\bar{r} > 0$. Then, $\hat{f}$ is a radial function and we have*

$$\hat{f}(r) = \alpha + (\beta - \alpha)\chi_{(\hat{r},\bar{r})}(r), \quad r \in [0, \bar{r}], \quad \textit{where} \quad \hat{r} = \left(\bar{r}^N - \frac{A}{\omega_N}\right)^{\frac{1}{N}},$$

and ω_N indicates the volume of the unit ball in $\mathbb{R}^N$.

Proof. Since Ω is Steiner symmetric with respect to all hyperplane T, the result is obtained in view of Theorem 3.4. $\square$

In the next theorem we will determine the optimizer when Ω is an annulus. It reveals that $\hat{D}^c$ is an annulus in Ω.

Theorem 3.6. *Let $\Omega = \mathcal{B}(\mathbf{0}, r_2) \setminus \mathcal{B}(\mathbf{0}, r_1)$ with $r_2 > r_1 > 0$ and assume $\alpha > 0$. Then, $\hat{f}$ is a radial function and there is $\delta > 0$ and $a \in (r_1 + \delta, r_2 - \delta)$ such that*

$$\hat{f}(r) = \alpha + (\beta - \alpha)\chi_{(r_1, a-\delta)\cup(a+\delta, r_2)}(r), \quad r \in [r_1, r_2],$$

where $|(\mathcal{B}(\mathbf{0}, a-\delta) \setminus \mathcal{B}(\mathbf{0}, r_1)) \cup (\mathcal{B}(\mathbf{0}, r_2) \setminus \mathcal{B}(\mathbf{0}, a+\delta))| = A$.

Proof. Assume that $\hat{f} = \alpha + (\beta - \alpha)\chi_{\hat{D}}$ is not a radial function. Rotating $\hat{D}$, one can find infinitely many minimizers which contradicts the uniqueness of the minimizer. Hence $\hat{f}$ is a radial function and $\hat{D}$ is radially symmetric. In view of the radial structure of $\hat{f}$, one can rewrite (1.1) as

$$\begin{cases} \left(r^{N-1}|\hat{u}'|^{p-2}\hat{u}'\right)' = -r^{N-1}\hat{f}(r) & r_1 < r < r_2, \\ u(r_1) = u(r_2) = 0. \end{cases} \tag{3.4}$$

An integration of (3.4) yields

$$r^{N-1}|\hat{u}'|^{p-2}\hat{u}'(r) = r_1^{N-1}\left(\hat{u}'(r_1)\right)^{p-2}\hat{u}'(r_1) - \int_{r_1}^{r} s^{N-1}\hat{f}(s)\mathrm{d}s, \tag{3.5}$$

in view of non-negativity of $\hat{u}'(r_1)$. Let $\bar{r} \in (r_1, r_2)$ be a maximizer of $\hat{u}(r)$. Then, $\hat{u}'(\bar{r}) = 0$ and so $\bar{r}$ is a solution of the following equation

$$g(r) := \int_{r_1}^{r} s^{N-1}\hat{f}(s)\mathrm{d}s = r_1^{N-1}\left(\hat{u}'(r_1)\right)^{p-2}\hat{u}'(r_1). \tag{3.6}$$

Indeed every $r \in (r_1, r_2)$ with $\hat{u}'(r) = 0$ is a solution of (3.6). But, the function $g : [r_1, r_2] \to \mathbb{R}$ is an increasing continuous function and hence $\bar{r}$ is the unique solution of (3.6). This reveals that the maximizer point of $\hat{u}(r)$ is unique. Now, (3.1) yields the assertion of the theorem. $\square$

We close this section with deriving the explicit formula of $\mathcal{F}(\hat{f})$ in case $N = 1$. Considering $\Omega = (-r, r)$ with $r > 0$, it is observed that $\hat{f}(x) = \alpha + (\beta - \alpha)\chi_{(-r,-\hat{x})\cup(\hat{x},r)}(x)$ with $\hat{x} = r - (A/2)$ according to Theorem 3.5. Then it is easy to check that

$$u_{\hat{f}}(x) = \frac{p-1}{\beta p} \tag{3.7}$$

$$\times\begin{cases} ((r-\hat{x})\beta+\alpha\hat{x})^{\frac{p}{p-1}}-(\alpha\hat{x})^{\frac{p}{p-1}}+\beta\alpha^{\frac{1}{p-1}}\left(\hat{x}^{\frac{p}{p-1}}-x^{\frac{p}{p-1}}\right) & 0<x<\hat{x},\\ -(x\beta+\hat{x}(\alpha-\beta))^{\frac{p}{p-1}}+(r\beta+\hat{x}(\alpha-\beta))^{\frac{p}{p-1}} & \hat{x}<x<r, \end{cases}$$

and $u_{\hat{f}}(-x)=u_{\hat{f}}(x)$. Therefore, one can calculate

$$\begin{aligned}\mathcal{F}(\hat{f})=\frac{2(p-1)}{\beta\,(2\,p-1)p}\Bigg(&(1-p)\,(\beta\,r+(\alpha-\beta)\,\hat{x})^{\frac{2\,p-1}{p-1}}\\ &+2\,(\beta\,r+(\alpha-\beta)\,\hat{x})\,(2\,p-1)\,(\beta\,r+(\alpha-\beta)\,\hat{x})^{\frac{p}{p-1}}\\ &+\hat{x}^{\frac{2\,p-1}{p-1}}\left((p-1)\,\alpha^{\frac{2\,p-1}{p-1}}+\alpha\left((-2\,p+1)\,\alpha^{\frac{p}{p-1}}+\alpha^{(p-1)^{-1}}\beta\,p\right)\right)\Bigg).\end{aligned}\tag{3.8}$$

3.3. Nearly optimal solutions

As we mentioned earlier, deriving an analytical solution for (1.3) is hard. So, we turn our attention to determine nearly optimal solutions which are approximations to the minimizer for specific ranges of the parameter values in the optimization problem. It is established that the corresponding nearly optimal sets are in good agreement with the set $\hat{D}$.

First, we turn to the case that $\epsilon=\beta-\alpha$ is small and $\alpha>0$, the low contrast regime. Let us assume that ψ is the solution of (1.1) with the right-hand side $f(\mathbf{x})\equiv\alpha>0$. For $s>0$, we denote by E_s the sub-level set $E_s=\{\mathbf{x}\in\Omega:\ \psi(\mathbf{x})<s\}$ of ψ. The following theorem says that when ϵ is small enough, the optimal domain is squeezed between two sub-level sets of ψ. Indeed, these sub-level sets are nearly optimal domains when the problem is in low contrast regime.

Theorem 3.7. *Let τ be chosen such $|E_\tau|=A$. For every $\delta>0$ there is ϵ_0 such that whenever $\epsilon<\epsilon_0$ and*

$$\hat{f}_\epsilon=\alpha+\epsilon\chi_{\hat{D}_\epsilon},\quad \textit{with}\quad \hat{D}_\epsilon=\{x\in\Omega:\ \hat{u}_\epsilon(\mathbf{x})<\hat{t}_\epsilon\},$$

is an optimal solution, then $|\hat{t}_\epsilon-\tau|<\delta$ and

$$E_{\tau-\delta}\subset\hat{D}_\epsilon\subset E_{\tau+\delta}.$$

Proof. While $\epsilon\to0$, it is easy to check that $\|\hat{u}_\epsilon\|_{W_0^{1,p}(\Omega)}$ is bounded in view of (2.1). The compact embedding of $W_0^{1,p}(\Omega)$ into $L^p(\Omega)$ (see [20]) yields that there is $\hat{u}$ in $W_0^{1,p}(\Omega)$ such that

$$\hat{u}_\epsilon\rightharpoonup\hat{u},\quad\text{in}\quad W_0^{1,p}(\Omega),\qquad \hat{u}_\epsilon\to\hat{u}\quad\text{in}\quad L^p(\Omega),\tag{3.9}$$

whenever $\epsilon\to0$. Moreover, recall that $\hat{f}_\epsilon\to\alpha$ in $L^p(\Omega)$. Note that

$$\int_\Omega|\nabla\hat{u}_\epsilon|^{p-2}\nabla\hat{u}_\epsilon\cdot\nabla\phi\mathrm{d}\mathbf{x}=\int_\Omega\hat{f}_\epsilon\phi\mathrm{d}\mathbf{x},\tag{3.10}$$

for $\phi\in C_0^\infty(\Omega)$. Obviously, the right-hand side of (3.10) converges to $\alpha\int_\Omega\phi\mathrm{d}\mathbf{x}$ when $\epsilon\to0$. Next we show that the left-hand side of (3.10) converges to $\int_\Omega|\nabla\hat{u}|^{p-2}\nabla\hat{u}\cdot\nabla\phi\mathrm{d}\mathbf{x}$. Setting $\phi=\hat{u}_\epsilon-\hat{u}$ in (3.10) and subtracting $\int_\Omega|\nabla\hat{u}|^{p-2}\nabla\hat{u}\cdot\nabla(\hat{u}_\epsilon-\hat{u})$ from both sides, we have

$$\int_\Omega\left(|\nabla\hat{u}_\epsilon|^{p-2}\nabla\hat{u}_\epsilon-|\nabla\hat{u}|^{p-2}\nabla\hat{u}\right)\cdot\nabla(\hat{u}_\epsilon-\hat{u})\mathrm{d}\mathbf{x}$$

$$= \int_\Omega \hat{f}_\epsilon \hat{u}_\epsilon^{p-1}(\hat{u}_\epsilon - \hat{u})\mathrm{d}\mathbf{x} - \int_\Omega |\nabla \hat{u}|^{p-2}\nabla \hat{u} \cdot \nabla(\hat{u}_\epsilon - \hat{u})\mathrm{d}\mathbf{x}. \tag{3.11}$$

We show that both integrals on the right-hand side converge to zero as $\epsilon \to 0$. For the first one by Hölder's inequality it is inferred that $\left|\int_\Omega \hat{f}_\epsilon \hat{u}_\epsilon^{p-1}(\hat{u}_\epsilon - \hat{u})\mathrm{d}\mathbf{x}\right| \le C(\alpha+\epsilon)^2\|\hat{u}_\epsilon - \hat{u}\|_{L^1(\Omega)}$, and so the integral converges to zero invoking (3.9). Furthermore, the second integral converges to zero because of the weak convergence in (3.9). Then, we infer that

$$\lim_{\epsilon\to 0}\int_\Omega \left(|\nabla \hat{u}_\epsilon|^{p-2}\nabla \hat{u}_\epsilon - |\nabla \hat{u}|^{p-2}\nabla \hat{u}\right)\cdot \nabla(\hat{u}_\epsilon - \hat{u})\mathrm{d}\mathbf{x} = 0. \tag{3.12}$$

Recall the following well-known inequalities

$$(\|\mathbf{A}\|^{p-2}\mathbf{A} - \|\mathbf{B}\|^{p-2}\mathbf{B}, \mathbf{A}-\mathbf{B}) \ge \begin{cases} C_1\|\mathbf{A}-\mathbf{B}\|^p & p \ge 2, \\ C_2\frac{\|\mathbf{A}-\mathbf{B}\|^2}{(\|\mathbf{A}\|+\|\mathbf{B}\|)^{2-p}} & 1 < p \le 2, \end{cases}$$

where $(.,.)$ denotes the usual inner product in $\mathbb{R}^N$, and $\mathbf{A},\mathbf{B} \in \mathbb{R}^N$. Consequently from (3.12), it is deduced by these inequalities that

$$\lim_{\epsilon\to 0}\int_\Omega |\nabla \hat{u}_\epsilon - \nabla \hat{u}|^p \mathrm{d}\mathbf{x} = 0. \tag{3.13}$$

Therefore, we can pass to the limit under the integral sign in (3.10) and then we have

$$-\Delta_p \hat{u} = \alpha, \quad \text{in } \Omega, \quad \hat{u} = 0 \quad \text{on } \partial\Omega.$$

This means that indeed $\hat{u} = \psi$. Now, (3.13) and well known Sobolev inequalities, Theorem 7.10 in [20], implies that $\lim_{\epsilon\to 0}\|\hat{u}_\epsilon - \psi\|_{L^\infty(\Omega)} = 0$.

Let us choose ϵ_0 such that $\|\hat{u}_\epsilon - \psi\|_{L^\infty(\Omega)} < \delta/2$ for all $\epsilon \le \epsilon_0$. Assume $\mathbf{x}$ belongs to $\hat{D}_\epsilon$ then we have $\hat{u}_\epsilon(\mathbf{x}) < \hat{t}_\epsilon$ and then $\psi(\mathbf{x}) < \hat{t}_\epsilon + \delta/2$, and hence $\hat{D}_\epsilon \subset E_{\hat{t}_\epsilon+\delta/2}$. Similarly, it is established that $E_{\hat{t}_\epsilon-\delta/2} \subset \hat{D}_\epsilon$. Consequently, we observe that

$$E_{\hat{t}_\epsilon-\delta/2} \subset \hat{D}_\epsilon \subset E_{\hat{t}_\epsilon+\delta/2},$$

which yields $|E_{\hat{t}_\epsilon-\delta/2}| \le A \le |E_{\hat{t}_\epsilon+\delta/2}|$.

We know that the level sets of ψ are of zero measure. Then, it is easy to check that $|E_s|$ is continuous with respect to s. By the continuity, there exists τ such that $|E_\tau| = A$ and $|\tau - \hat{t}_\epsilon| < \delta/2$. Collecting all of above results, we obtain the assertions of the theorem. □

The other interesting case is to consider $p \to \infty$. For every $\mathbf{x} \in \bar{\Omega}$, the distance function is defined $\mathrm{dist}(\mathbf{x}) = \inf_{\mathbf{y}\in\partial\Omega}\|\mathbf{x}-\mathbf{y}\|_2$. For $s > 0$, we denote by F_s the sub-level set $F_s = \{\mathbf{x} \in \Omega : \mathrm{dist}(\mathbf{x}) < s\}$. Then, the next theorem asserts that sub-level sets of the distance function are nearly optimal domain when p is large enough.

Theorem 3.8. *Let τ be chosen such $|F_\tau| = A$ and $\alpha > 0$.*
a) For every $\delta > 0$ there is p_0 such that whenever $p > p_0$ and

$$\hat{f}_p = \alpha + (\beta-\alpha)\chi_{\hat{D}_p}, \quad \textit{with} \quad \hat{D}_p = \{\mathbf{x} \in \Omega : \hat{u}_p(\mathbf{x}) < \hat{t}_p\},$$

is an optimal solution corresponding to p, then $|\hat{t}_p - \tau| < \delta$ *and*

$$F_{\tau-\delta} \subset \hat{D}_p \subset F_{\tau+\delta}.$$

b) We have

$$\lim_{p\to+\infty} \mathcal{F}(\hat{f}_p) = \int_\Omega (\alpha + (\beta-\alpha)\chi_{F_\tau})\, dist(\mathbf{x})\mathrm{d}\mathbf{x}. \tag{3.14}$$

Proof. (a) Recall that $\hat{u}_p$ is the unique solution of

$$-\Delta_p u = \hat{f}_p \quad \text{in } \Omega, \quad u = 0 \quad \text{on } \partial\Omega.$$

Then, we have

$$\lim_{p\to\infty} \hat{u}_p(\mathbf{x}) = \mathrm{dist}(\mathbf{x}), \quad \text{in} \quad C^r(\bar{\Omega}) \quad \text{for all} \quad r \in (0,1), \tag{3.15}$$

see Proposition 2.1 and Remark 2.1 in [6]. Moreover, it is well-known that $\mathrm{dist}(\mathbf{x}) \in W_0^{1,p}(\Omega)$ for $p > N$ and it is the unique viscosity solution of $|\nabla v| = 1$ in Ω, see [15]. Hence, the level sets of $\mathrm{dist}(\mathbf{x})$ are of zero measure in view of Lemma 7.7 in [20]. Now, employing the uniform convergence in (3.15), the reminder of the proof is similar to that of Theorem 3.7 and is omitted.
(b) Let $\{p_n\}$ be a sequence of positive numbers such that $p_n \to +\infty$. Set $f_n = \hat{f}_{p_n}$ and $u_n = \hat{u}_{p_n}$. Remember that since f_n belongs to $\mathcal{N}$, then we have $\|f_n\|_{L^2(\Omega)} = \|f_0\|_{L^2(\Omega)}$ for all $n \to \infty$. Thus, we infer that there is a subsequence, still denoted by $\{f_n\}$, and $f^\infty \in \mathcal{M}$ such that

$$f_n \rightharpoonup f^\infty \quad \text{in} \quad L^2(\Omega). \tag{3.16}$$

One can obtain

$$\int_\Omega f_n u_n - f^\infty \mathrm{dist}\, \mathrm{d}\mathbf{x} = \int_\Omega f_n(u_n - \mathrm{dist})\mathrm{d}\mathbf{x} + \int_\Omega (f_n - f^\infty)\mathrm{dist}\, \mathrm{d}\mathbf{x}. \tag{3.17}$$

While, $n \to \infty$, the first integral on the right-hand side of (3.17) converges to zero in view of (3.15) and the fact that $\|f_n\|_{L^2(\Omega)} = \|f_0\|_{L^2(\Omega)}$. The second one converges to zero due to (3.16). Hence, we find that

$$\lim_{n\to+\infty} \mathcal{F}(f_n) = \int_\Omega f^\infty \mathrm{dist}(\mathbf{x})\mathrm{d}\mathbf{x}.$$

Recall that f_n is the unique minimizer of $\mathcal{F}$ relative to $\mathcal{N}$ for $p = p_n$. Indeed it is a minimizer relative to $\mathcal{M}$ due to the weak continuity of the functional $\mathcal{F}$, see Lemma 2.1. Now in view of Lemma 2.2, it is inferred that

$$\int_\Omega f_n u_n \mathrm{d}\mathbf{x} \le \int_\Omega f u_n \mathrm{d}\mathbf{x}, \quad \text{for every} \quad f \in \mathcal{M}.$$

Passing to limit in the above inequality yields

$$\int_\Omega f^\infty \mathrm{dist}\, \mathrm{d}\mathbf{x} \le \int_\Omega f \mathrm{dist}\, \mathrm{d}\mathbf{x}, \quad \text{for all} \quad f \in \mathcal{M},$$

TABLE 1. Explicit formula of the torsion function.

Ω	$\{\frac{x^2}{a^2}+\frac{y^2}{b^2}<1\}$	$\{y+\frac{2a}{\sqrt{3}}>0,\ \sqrt{3}\lvert x\rvert<y-\frac{a}{\sqrt{3}}\}$
$\psi(x,y)$	$\frac{\left(1-\frac{x^2}{a^2}-\frac{y^2}{b^2}\right)}{2\left(\frac{1}{a^2}+\frac{1}{b^2}\right)}$	$\frac{1}{4\sqrt{3}a}\left(y+\frac{a}{\sqrt{3}}\right)\left(\left(y-\frac{2a}{\sqrt{3}}\right)^2-3x^2\right)$

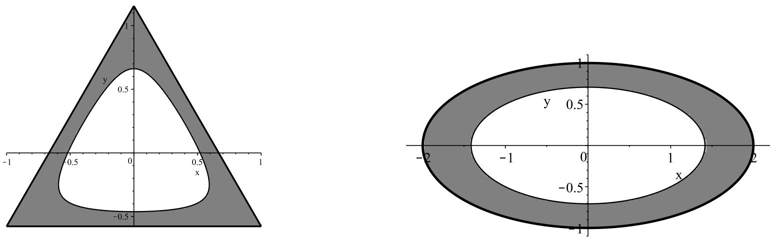

(a) (b)

FIGURE 1. Nearly optimal solutions in the low contrast regime with $p=2$. The set E_τ with $|E_\tau|=|\Omega|/2$ is shown in gray.

and so f^∞ is the unique minimizer of the functional $L(f)=\int_\Omega f\mathrm{dist}\,\mathrm{d}\mathbf{x}$ relative to $f\in\mathcal{M}$. On the other-hand, since the level sets of $\mathrm{dist}(\mathbf{x})$ are of zero measure one can define non-increasing function $\zeta(s)$ where $\zeta(s)=\beta$ for $s<\tau$ and $\zeta(s)=\alpha$ when $s\geq\tau$ such that $\zeta(\mathrm{dist}(\mathbf{x}))=\alpha+(\beta-\alpha)\chi_{F_\tau}$ belongs to $\mathcal{N}$. Lemma 2.3 reveals that $\zeta(\mathrm{dist}(\mathbf{x}))$ is the unique minimizer of $L(f)$ and so we should have $f^\infty=\alpha+(\beta-\alpha)\chi_{F_\tau}$. This completes the proof. □

Remark 3.9. Investigating the asymptotic case $p\to 1$ is tricky. Fix the right-hand side $f(\mathbf{x})$ in (1.1). Depending on the size and shape of Ω and the norm of $f(\mathbf{x})$, it has been proved that solutions u_p of the equation could converge to zero, to a characteristic function of Ω or diverge to $+\infty$ when $p\to 1$ [13, 32, 33, 39]. For one-dimensional domain $\Omega=(-r,r)$, formula (3.7)–(3.8) indicate the behavior of $u_{\hat f}$ and $\mathcal{F}(\hat f)$ when $p\to 1$. Setting $\alpha=1,\beta=2,\hat x=\frac{1}{2}$ and $r=\frac{3}{4}$ in (3.7)–(3.8), we observe that $u_{\hat f}\to 0$ uniformly and $\mathcal{F}(\hat f)\to 0$ while $p\to 1$. If we replace the value of r with 2, we observe that $u_{\hat f}\to+\infty$ and so $\mathcal{F}(\hat f)\to+\infty$ whenever $p\to 1$. It reveals the effect of size of the domain on the asymptotic behaviors. Setting $\alpha=\frac{1}{3},\beta=\frac{2}{3},\hat x=\frac{1}{2}$ and $r=1$ in (3.7)–(3.8), we find that $u_{\hat f}\to 0$ uniformly and $\mathcal{F}(\hat f)\to 0$ while $p\to 1$. If we replace the value of β with 2, we observe that $u_{\hat f}\to+\infty$ and so $\mathcal{F}(\hat f)\to+\infty$ whenever $p\to 1$. One can infer that the asymptotic behaviors depends on $\|\hat f\|_{L^\infty(\Omega)}$.

Although the analytical formula for optimal domains is quite rare, we can find such formula for nearly optimal domains when Ω is easy to describe. Consider problem (1.1) in the low contrast regime and set $p=2$, then indeed ψ is the solution of the (St Venant) elastic torsion problem and is called the torsion function. Explicit formula of the torsion functions of several curvilinear polygon are available [34]. Hence, the nearly optimal solutions can be derived analytically for such domains. For instance, we can find the explicit formula of the torsion function when $\alpha=1$ for an ellipse and an equilateral triangle in Table 1. Using function $\psi(x,y)$ in Table 1, one can easily find nearly optimal solution analytically for an ellipse and an equilateral triangle. For these domains a typical nearly optimal solution E_τ with $|E_\tau|=|\Omega|/2$ is depicted in Figure 1.

Nearly optimal solutions can be obtained analytically when $p\to\infty$ for domains that $\mathrm{dist}(\mathbf{x})$ can be calculated explicitly. For example, this function has an explicit formula when $\Omega\subset\mathbb{R}^2$ is a circle, rectangle, square, annulus,

TABLE 2. Explicit formula of $\operatorname{dist}(x, y)$.

Ω	$\{-a < x < a,\ -a < y < a\}$	$\{R_1 < x^2 + y^2 < R_2\}$
$\operatorname{dist}(x, y)$	$a - \frac{1}{2}\left(\lvert x\rvert + \lvert y\rvert + \lvert\lvert x\rvert - \lvert y\rvert\rvert\right)$	$\frac{1}{2}(R_2 - R_1)$ $\frac{-1}{2}\left\lvert R_2 + R_1 - 2\sqrt{x^2+y^2}\right\rvert$
$\lim_{p\to+\infty} \mathcal{F}(\hat{f}_p)$	$(4/3)\alpha a^3 + 4\tau^2(\beta-\alpha)(a - (2\tau/3))$	$(\alpha\pi/4)(R_1 - R_2)^2(R_1 + R_2)$ $+2\pi(\beta-\alpha)\tau^2(R_1 + (2\tau/3))$

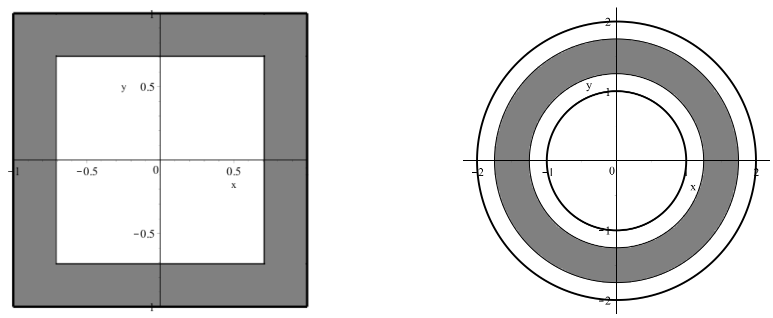

(a) (b)

FIGURE 2. Nearly optimal solutions when $p \to \infty$. The set F_τ with $|F_\tau| = |\Omega|/2$ is shown in gray.

ellipse, etc. In Table 2, one can find the explicit formula of $\operatorname{dist}(\mathbf{x})$ for a square and annulus. Moreover, one can find the value of $\mathcal{F}(\hat{f}_p)$ while $p \to \infty$ in the table. For these domains a typical nearly optimal domain F_τ with $|F_\tau| = |\Omega|/2$ is depicted in Figure 2.

4. Numerical algorithm

As explained earlier, analytical solutions for optimization problems of type (1.3) are quite rare. Therefore, it is necessary from physical point of view to develop a numerical algorithm to determine solutions of (1.3). Based upon rearrangement techniques, we will find sequence of functions $\{f_i\}_0^\infty \in \mathcal{N}$ where the corresponding energies $\{\mathcal{F}(f_i)\}_0^\infty$ is decreasing. The numerical algorithm is a modification of the methods developed in [27, 28, 41]. The following theorem provides the main tool for generating the minimizing sequence.

Theorem 4.1. *Let $f_i = \alpha + (\beta - \alpha)\chi_{D_i}$ and $f_{i+1} = \alpha + (\beta-\alpha)\chi_{D_{i+1}}$ with $|D_i| = |D_{i+1}| = A$ where u_i and u_{i+1} are the corresponding solutions of (1.1) respectively. If $|D_{i+1}\Delta D_i|$ is small enough and $\int_{D_{i+1}} u_i \mathrm{d}\mathbf{x} < \int_{D_i} u_i \mathrm{d}\mathbf{x}$, then we have $\mathcal{F}(f_{i+1}) < \mathcal{F}(f_i)$.*

Proof. Recall that functional $\mathcal{F}$ is continuously differentiable in view of Lemma 2.1. Indeed, the functional is Fréchet differentiable at f since the Gâteaux derivative is continuous at f, see Proposition 5.3.4 of [22]. Then, we see that

$$\begin{aligned}\mathcal{F}(f_{i+1}) - \mathcal{F}(f_i) &= \mathcal{F}\left(f_i + (f_{i+1} - f_i)\right) - \mathcal{F}(f_i) \\ &= q\int_\Omega (f_{i+1} - f_i)u_i \mathrm{d}\mathbf{x} + o\left(\|f_{i+1} - f_i\|_{L^q(\Omega)}\right). \end{aligned} \tag{4.1}$$

It is observed that

$$\begin{aligned}\|f_{i+1}-f_i\|^q_{L^q(\Omega)} &= (\beta-\alpha)^q\int_\Omega |\chi_{D_{i+1}}-\chi_{D_i}|^q \mathrm{d}\mathbf{x} = (\beta-\alpha)^q\int_\Omega \chi_{D_{i+1}\Delta D_i}\mathrm{d}\mathbf{x}\\ &= (\beta-\alpha)^q|D_{i+1}\Delta D_i|.\end{aligned} \tag{4.2}$$

Therefore, when $|D_{i+1}\Delta D_i|$ is small enough (4.1) yields the assertion of the theorem in view of fact that

$$\int_\Omega (f_{i+1}-f_i)u_i\mathrm{d}\mathbf{x} = (\beta-\alpha)\left(\int_{D_{i+1}} u_i\mathrm{d}\mathbf{x} - \int_{D_i} u_i\mathrm{d}\mathbf{x}\right) < 0.$$

□

Based upon Theorem 3.2, we develop Algorithm 1. By employing Algorithm 1, one can obtain the sequence of functions $\{f_i\}_1^\infty \subset \mathcal{N}$ which converges to the solution of (1.3).

Theorem 4.2. *For the sequence $\{f_i\}_1^\infty$ derived by Algorithm 1, we have $f_i \to \hat{f}$ in $L^2(\Omega)$.*

Proof. Since $\{f_i\}_1^\infty \subset \mathcal{N}$, we know that $\|f_i\|_{L^2(\Omega)} = \|f_1\|_{L^2(\Omega)}$ for all $i\in\mathbb{N}$. Then, there is a subsequence (still denoted by $\{f_i\}_1^\infty$) and $\check{f}\in\mathcal{M}$ such that $f_i \rightharpoonup \check{f}$ in $L^2(\Omega)$. Indeed, we have

$$\mathcal{F}(\check{f}) = \inf_{i\in\mathbb{N}} \mathcal{F}(f_i). \tag{4.3}$$

The function $\check{f}$ is a minimum of functional $L(f) = \int_\Omega f u_{\check{f}}\mathrm{d}\mathbf{x}$ over $\mathcal{M}$ since if there is $g\in\mathcal{M}$ such that $L(g) < L(\check{f})$, then in view of Theorem 4.1 we can find $f\in\mathcal{N}$ such that $\mathcal{F}(f) < \mathcal{F}(\check{f})$ which contradicts (4.3). Therefore, we conclude that $\check{f}$ is a minimizer of (1.3) because of the optimality condition in Lemma 2.2. Furthermore, $\check{f} = \hat{f}$ due to the uniqueness in Theorem 3.1. Now, the Radón-Riesz Theorem reveals that $f_i \to \hat{f}$ in $L^2(\Omega)$. □

4.1. Numerical results

To solve (1.3) numerically using Algorithm 1, we start with an initial choice of f and modify f at each iteration to decrease the objective functional $\mathcal{F}$ until it reaches the minimum. The algorithm consists of two essential calculations. One is to find the solution u of equation (1.1) for any given f *via* a standard finite element

Algorithm 1 Minimization algorithm

Given α,β,p, A and TOL, choose an initial $f^{(0)}\in\mathcal{N}_{\alpha,\beta,A}$.
1. Set $i=0$.
2. Compute u_i the solution of (1.1) and $\mathcal{F}(f_i)$ by using a finite element method.
3. Compute $D_{i+1} = \{\mathbf{x}\in\Omega:\ u_i(\mathbf{x}) < \check{t}\}$ where $\check{t} = \inf\{s:\ |\{\mathbf{x}\in\Omega:\ u_i(\mathbf{x}) < s\}| \geq A\}$, and f_{i+1}.
4. Set $A' = |D_i\backslash D_{i+1}|$.
5. While $\mathcal{F}(f_{i+1}) > \mathcal{F}(f_i)$ do
Set $D_1 = D_i\backslash D_{i+1}$, $D_2 = D_{i+1}\backslash D_i$. Compute
$t_1 = \sup\{s: |\{\mathbf{x}\in D_1:\ u_i(\mathbf{x}) \geq s\}| \geq A'\}, t_2 = \inf\{s: |\{\mathbf{x}\in D_2:\ u_i(\mathbf{x}) \leq s\}| \geq A'\}$.
Set $\tilde{D}_1 = \{\mathbf{x}\in D_1:\ u_i(\mathbf{x}) \geq t_1\}$, and $\tilde{D}_2 \subset \{\mathbf{x}\in D_2:\ u_i(\mathbf{x}) \leq t_2\}$ with $|D_2| = A'$.
Set $D_{i+1} = (D_i\backslash\tilde{D}_1)\cup\tilde{D}_2$ and $f_{i+1} = \beta\chi_{D_{i+1}} + \alpha\chi_{D^c_{i+1}}$.
Compute u_{i+1} and $\mathcal{F}(f_{i+1})$ by using a finite element method. Set $A' = A'/2$;
6. If $\|f_{i+1}-f_i\|_{L^2(\Omega)} < TOL$, stop the algorithm. Otherwise set $i=i+1$, go to step 2.

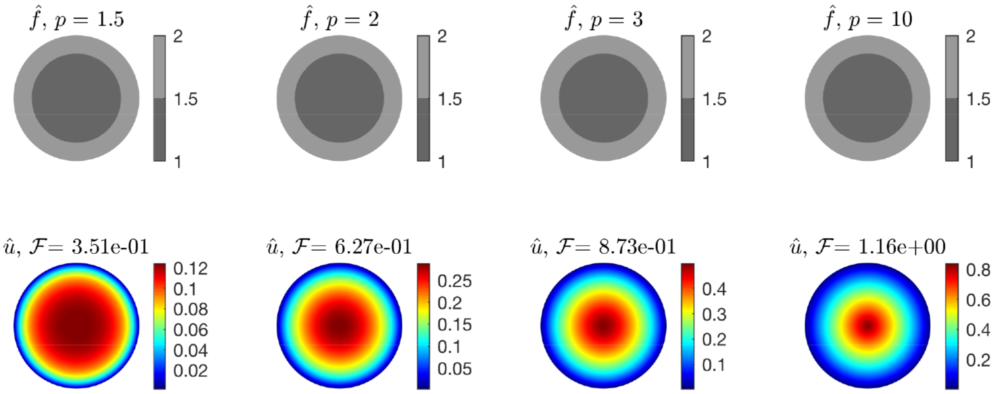

FIGURE 3. The minimizer $\hat{f}$ and its corresponding $\hat{u}$ on a disk for $p = 1.5, 2, 3, 10$.

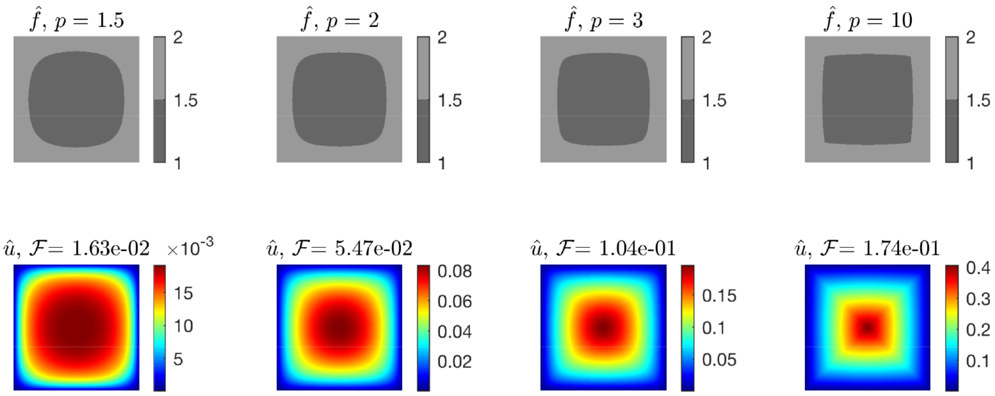

FIGURE 4. The minimizer $\hat{f}$ and its corresponding $\hat{u}$ on a square for $p = 1.5, 2, 3, 10$.

method while the other one is to determine a new f for any given u by a rearrangement algorithm so that the objective functional decreases.

In numerical implementations for two-phase problems, we choose $\alpha = 1$ and $\beta = 2$ unless otherwise specified. We first compute the distance function $\text{dist}(\mathbf{x})$ which is the solution of Equation (1.3) when $p \to \infty$. This can be estimated by taking the minimum among distance to all points sampled on the boundary $\partial\Omega$. Alternatively, one can also use fast marching [48] or fast sweeping methods [29, 52] to compute the solution of eikonal equation. When $p = 2$, equation (1.3) is linear and can be solved easily. Denote this solution by $\hat{u}_2$. When $p \neq 2$, the resulting nonlinear discretization of FEM method requires a good initial guess of the solution of (1.1) to ensure the convergence. We choose $u_p^{(0)} = \frac{1}{p-1}\hat{u}_2 + \frac{p-2}{p-1}\text{dist}(\mathbf{x})$ which is a convex combination of $\hat{u}_2$ and $\text{dist}(\mathbf{x})$ when $p \geq 2$ and $u_p^{(0)} = \hat{u}_2$ when $p < 2$. We then choose the initial f as $f = \alpha + (\beta - \alpha)\chi_D$ such that

$$D = \{\mathbf{x} \in \Omega : \; u_p^{(0)}(\mathbf{x}) < \hat{t}\}, \quad |D| = A.$$

In Figures 3–7, we show the numerical results for $p = 1.5, 2, 3, 10$ and $A = 0.5|\Omega|$ on a circle, a square, an L-shaped domain, a dumbbell, and an annulus. The triangular meshes used have $190,220$, $141,090$, $106,846$, $155,086$, and $268,314$ elements, respectively. The optimal set $\hat{D}$ corresponding to the optimizer $\hat{f}$ contains a tubular neighborhood of the boundary $\partial\Omega$ as discussed in Theorem 3.3. In particular, if $\Omega \subset \mathbb{R}^2$ is simply connected, we have $\hat{D}$ is connected as shown in Figures 3–6. However, $\hat{D}$ has two connected components on an annulus in Figure 7 as an annulus is not simply-connected. The solution $u_{\hat{f}}$ is approaching to the distance

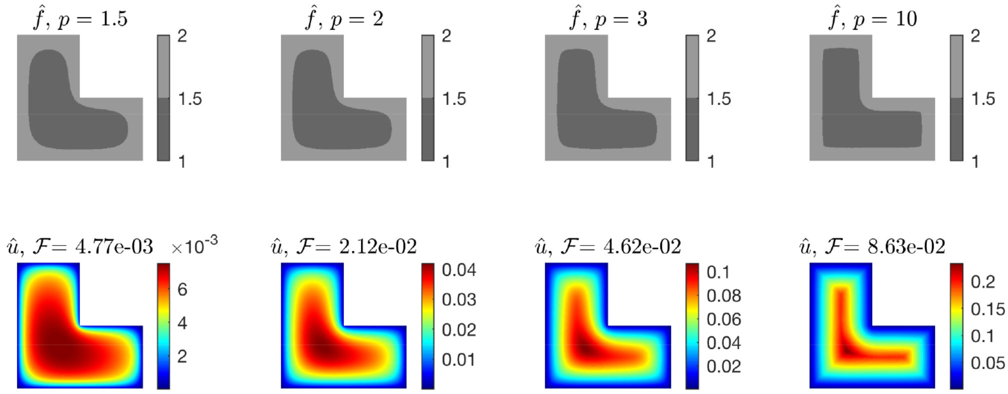

FIGURE 5. The minimizer $\hat{f}$ and its corresponding $\hat{u}$ on a L-shaped domain for $p = 1.5, 2, 3, 10$.

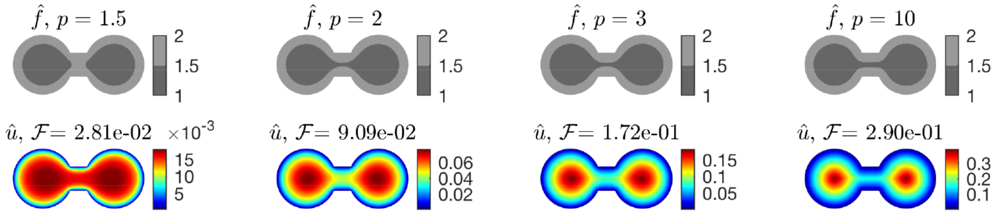

FIGURE 6. The minimizer $\hat{f}$ and its corresponding $\hat{u}$ on an annulus for $p = 1.5, 2, 3, 10$.

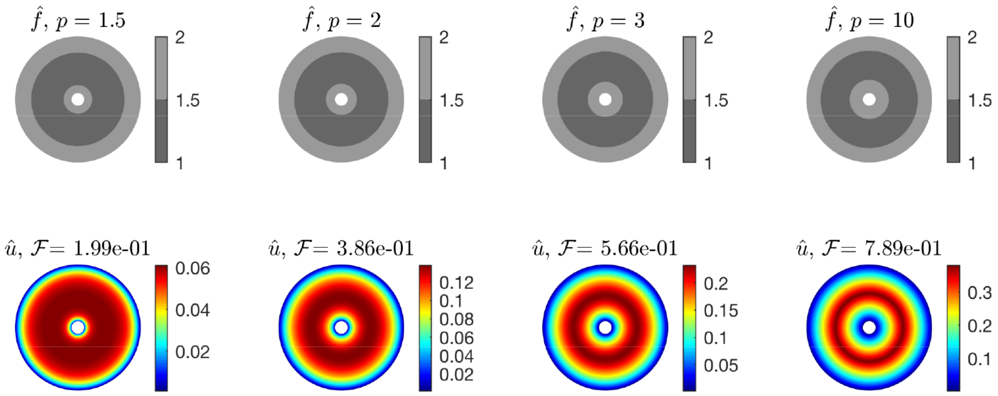

FIGURE 7. The minimizer $\hat{f}$ and its corresponding $\hat{u}$ on an annulus for $p = 1.5, 2, 3, 10$.

function when $p \to \infty$. On a circle in Figure 3, the optimal solution is $\hat{f}(r) = 1 + \chi_{(\frac{1}{\sqrt{2}},1)}(r), r \in [0, 1]$ regardless of the value of p. This demonstrates a consistency with Theorem 3.5. In Figure 4, the optimizer on a square has $\hat{D}^c$ approaching to a square with a width $\frac{1}{\sqrt{2}}$ when $p \to \infty$. In Figure 5, the optimizer on the L-shaped domain has $\hat{D}^c$ which is a resulting shape of a morphological erosion by a disk for large p. On an annulus with the inner radius 0.1 and the outer radius 1, the optimizer $\hat{f}$ in Figure 7 is a radial function and $\hat{D}^c$ is an annulus as discussed in Theorem 3.6. Note that the optimizer $\hat{f}$ varies with respect to p. The $\hat{D}$ consists of two rings attached to the inner and outer boundaries. The inner ring is thinner than the outer ring when p is finite. When $p \to \infty$, the solution $\hat{u}$ becomes a distance function and the thicknesses of two rings are the same.

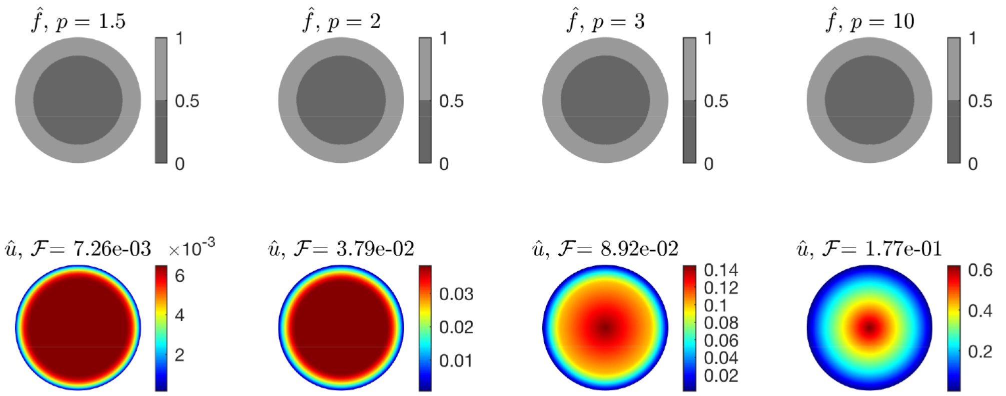

FIGURE 8. The minimizer $\hat{f}$ and its corresponding $\hat{u}$ on a disk for $p = 1.5, 2, 3, 10$.

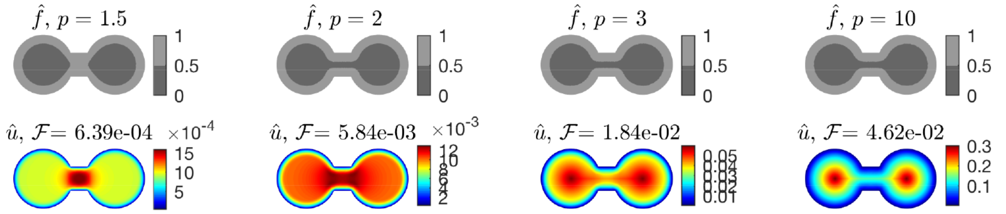

FIGURE 9. The minimizer $\hat{f}$ and its corresponding $\hat{u}$ on an annulus for $p = 1.5, 2, 3, 10$.

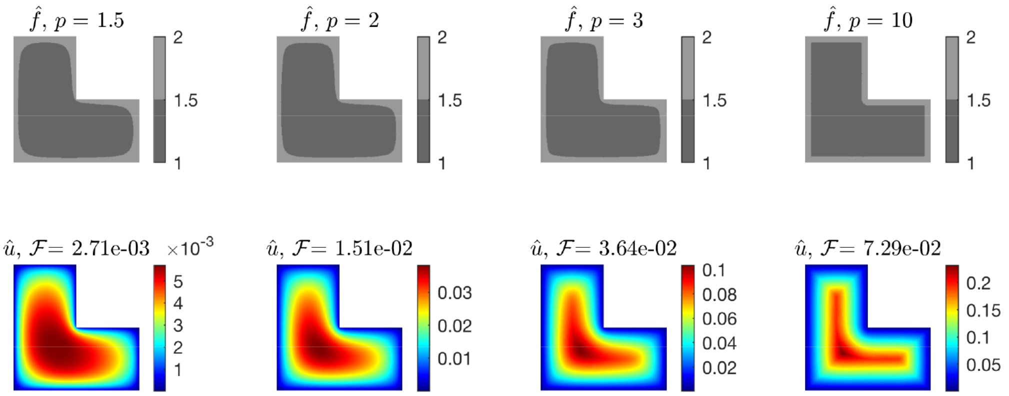

FIGURE 10. The minimizer $\hat{f}$ and its corresponding $\hat{u}$ on a L-shaped domain for $p = 1.5, 2, 3, 10$.

Figures 8 and 9 show the numerical results for $p = 1.5, 2, 3, 10$ and $A = 0.5|\Omega|$ on a circle and a dumbbell for $\alpha = 0$ and $\beta = 1$. The solutions $\hat{u}$ and $\hat{f}$ are both radial symmetric on the circular domain as shown in Figure 8. Also, we observed that, u is constant in the region where $\hat{f} = 0$ for $p \leq 2$. For $p = 2$, u is a quadratic function in r in the region where $\hat{f} = 1$. In Figure 9, we observed that $\hat{f}$ may have different topology and $\hat{u}$ is not constant in the region where $\hat{f} = 0$ for $p \leq 2$ anymore. When $p = 1.5$, the function $\hat{u}$ has one global maximum. However, $\hat{u}$ approaches to a distance function which has two maximums on a dumbbell as $p \to \infty$.

In Figure 10 and 11, the numerical results for $p = 1.5, 2, 3, 10$ on the L-shaped domain are shown for $A = 0.25|\Omega|$ and $A = 0.75|\Omega|$, respectively. We observe that $\mathcal{F}$ is increasing in $|A|$ which is what we expect from Theorem 3.2. Again, the solution $\hat{u}$ is approaching to the distance function when $p \to \infty$.

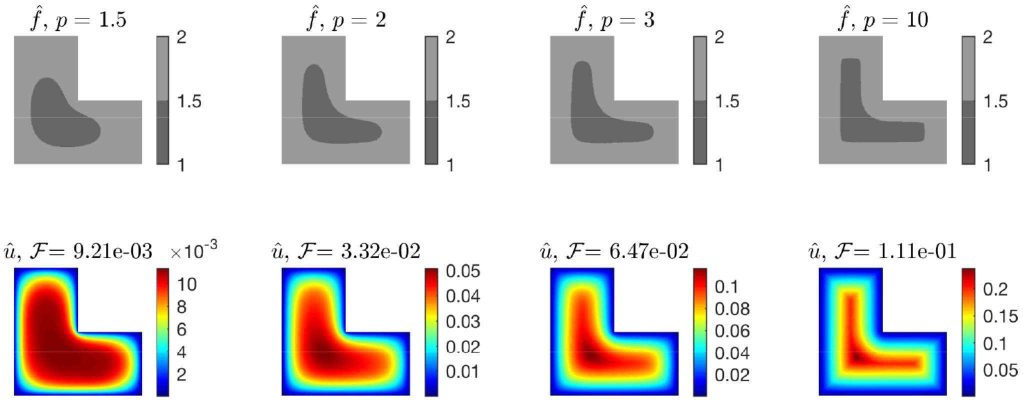

FIGURE 11. The minimizer $\hat{f}$ and its corresponding $\hat{u}$ on a L-shaped domain for $p = 1.5, 2, 3, 10$.

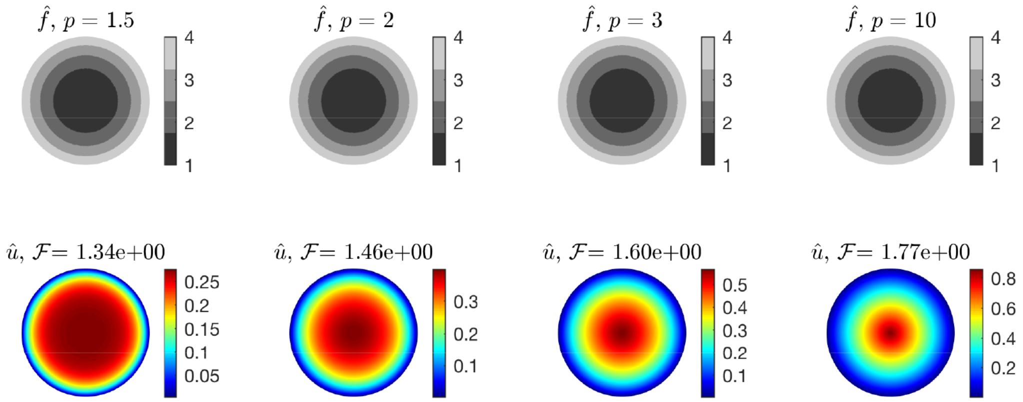

FIGURE 12. The minimizer $\hat{f}$ and its corresponding $\hat{u}$ on a disk for $p = 1.5, 2, 3, 10$.

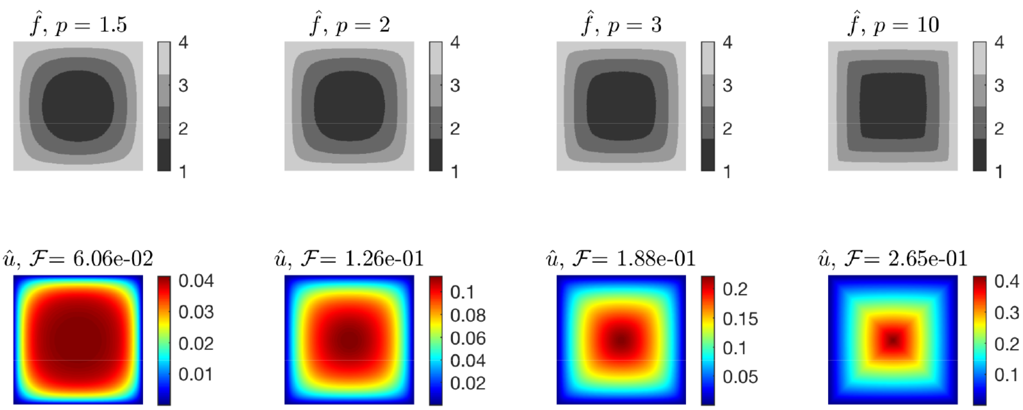

FIGURE 13. The minimizer $\hat{f}$ and its corresponding $\hat{u}$ on a square for $p = 1.5, 2, 3, 10$.

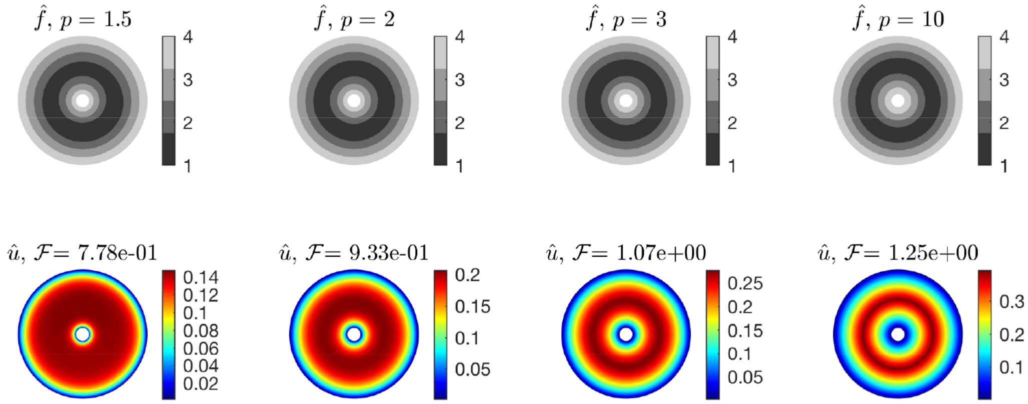

FIGURE 14. The minimizer $\hat{f}$ and its corresponding $\hat{u}$ on an annulus for $p = 1.5, 2, 3, 10$.

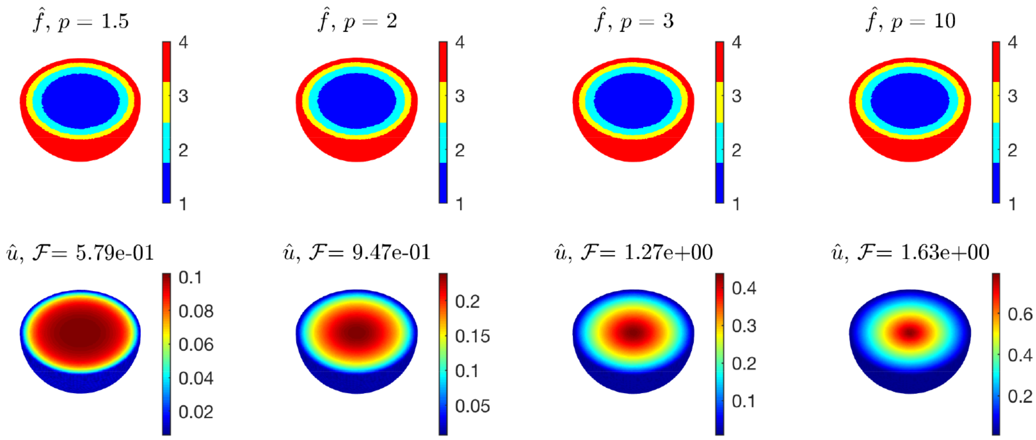

FIGURE 15. The minimizer $\hat{f}$ and its corresponding $\hat{u}$ on the unit sphere for $p = 1.5, 2, 3, 10$.

The aforementioned algorithm for the two-phase problem can be easily extended to the n-phase problem. Assume that f can take n different values: α_i, $1 \leq i \leq n$ and

$$D_i = \{x | f_i(x) = \alpha_i\},$$

satisfies $|D_i| = A_i$ with $\sum_{i=1}^{i=n} A_i = |\Omega|$. When a solution u of (1.1) is obtained, the rearrangement is chosen as $f_{\text{new}} = \sum_{i=1}^{n} \alpha_i \chi_{D_i}$ where D_i is determined by

$$\cup_{i=1}^{j} D_i = \{\mathbf{x} \in \Omega : \ u_f(\mathbf{x}) \leq t_j\}, \quad \left|\cup_{i=1}^{j} D_i\right| = \sum_{i=1}^{j} A_i, \quad 1 \leq i \leq n, \quad 1 \leq j \leq n.$$

In Figures 12–14, we show the results for a four-phase problem, *i.e.*, $n = 4$ with $A_i = \frac{|\Omega|}{4}$, on different domains. We observe that D_i, $1 \leq i \leq n$, are nested for every optimizer. When $p \to \infty$, the solution $\hat{u}$ is approaching to a distance function to $\partial\Omega$. The interface between different D_i approaches to level contours of the corresponding distance function.

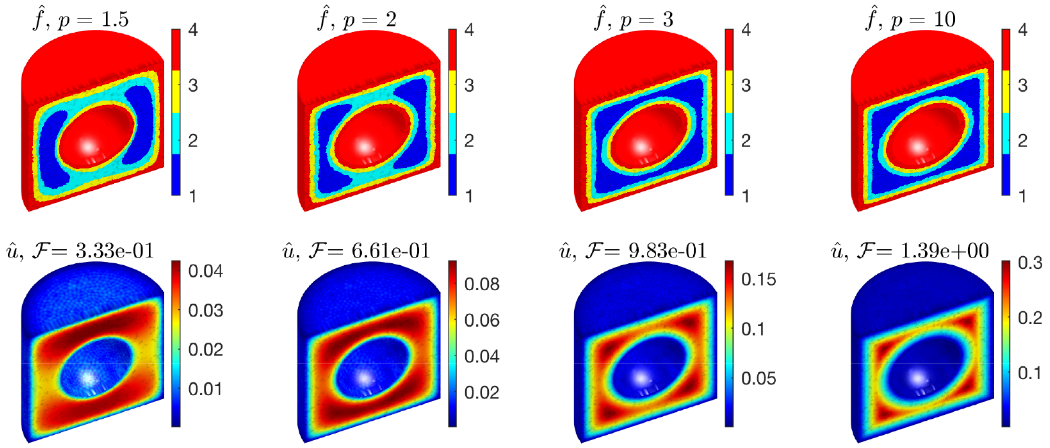

FIGURE 16. The minimizer $\hat{f}$ and its corresponding $\hat{u}$ on a cylinder with a hole for $p = 1.5, 2, 3, 10$.

In Figure 15–16, the computation on tetrahedron meshes of an unit sphere and a cylinder with a hole are shown. The tetrahedron meshes are generated by using the DistMesh package [45]. The unit sphere has $158,277$ of tetrahedrons while the cylinder with a hole has $225,028$ ones. We show the numerical results for $p = 1.5, 2, 3, 10$ for a four-phase problem with $A_i = \frac{|\Omega|}{4}$. In order to visualize the solutions, we show the domain for $z < 0$ for the unit sphere and $x < 0$ for the cylinder with a hole. The nesting behaviors of different phases in f are interesting. Sets D_1 and D_2 change their topologies from $p = 2$ to $p = 3$ in Figure 16. When $p \to \infty$, the solution $\hat{u}$ is again approaching to a distance function to $\partial\Omega$.

5. Conclusion

In this paper, we have studied the minimization problem corresponding to the p-Laplacian equation. We first have obtained the existence and uniqueness of a solution for the optimization problem. Second, we have shown monotonicity of the objective functional and found geometrical properties of the minimizer on a bounded domain in $\mathbb{R}^N$. In particular, we derived the analytic radial solution when the domain is a ball or an annulus. However, finding an analytical solution for even geometrically simple domains such as rectangles and ellipses remains as an open problem. This is the reason that we turned our attention to determine nearly optimal solutions which are approximations to the minimizer for specific ranges of the parameter values in the optimization problem. It established that the corresponding nearly optimal sets are in good agreement with the set $\hat{D}$. We studied the nearly optimal solution in the low contrast regime by using rearrangement techniques. The nearly optimal solution is determined in view of the fact that u approaches to the solution of the torsion problem when $p = 2, (\beta - \alpha) \to 0$ and the explicit formula for the nearly optimal solution can be derived on domains such as an ellipse and an equilateral triangle. When $p \to \infty$, the solution u approaches to a distance function and so analytical formulas of the nearly optimal solution can be obtained on domains such as a square or an annulus.

At last, for general domains, we developed an efficient and robust rearrangement algorithm which converges to the corresponding optimizers in just a few iterations. Not only two-phase problems are studied but also numerical results on n-phase problems with $n = 4$ are shown. We invoked the algorithm to find the optimizer even for three-dimensional problems.

Physically, the optimizers that we have found in this paper for two-dimensional problems determine a pattern for exerting a force with a given amount of total energy in a way that the total displacement is minimal. Our results in this paper provide realistic insights on performance of membranes which are a building block in structural mechanics.

References

[1] P.R. Antunes, S.A. Mohammadi and H. Voss, A nonlinear eigenvalue optimization problem: optimal potential functions. *Nonlinear Anal.: Real World Appl.* **40** (2018) 307–327.

[2] C. Atkinson and C. Champion, On some boundary value problems for the equation$\nabla\cdot$ (f($|\nabla$w$|$)∇w)= 0. *Proc. Royal Soc. Lond. Math. Phys. Sci.* **448** (1995) 269–279.

[3] K. Atkinson and W. Han, Vol. 39 of Theoretical Numerical Analysis: A Functional Analysis Framework. Springer Science & Business Media (2009).

[4] F. Bahrami, B. Emamizadeh and A. Mohammadi, Existence of an extremal ground state energy of a nanostructured quantum dot. *Nonlinear Anal.: Theory Methods Appl.* **74** (2011) 6287–6294.

[5] F. Bahrami and H. Fazli, Optimization problems involving Poisson's equation in R^3. *Electr. J. Differ. Equ.* **2011** (2011) 1–9.

[6] T. Bhattacharya, E. DiBenedetto and J. Manfredi, Limits as p$\rightarrow\infty$ of $\delta_p u_p = f$ and related extremal problems. *Rend. Sem. Mat. Univ. Politec. Torino* **47** (1989) 15–68.

[7] H. Brezis, Functional analysis, Sobolev spaces and partial differential equations. Springer Science & Business Media (2010).

[8] F. Brock, Rearrangements and applications to symmetry problems in PDE. Vol. 4 of *Handbook of differential equations: stationary partial differential equations*. Elsevier (2007) 1–60.

[9] G. Burton, Rearrangements of functions, maximization of convex functionals, and vortex rings. *Math. Ann.* **276** (1987) 225–253.

[10] G. Burton, Variational problems on classes of rearrangements and multiple configurations for steady vortices. *Ann. Inst. Henri Poincaré (C) Non Linear Analysis* **6** (1989) 295–319.

[11] S. Chanillo, D. Grieser, M. Imai, K. Kurata and I. Ohnishi, Symmetry breaking and other phenomena in the optimization of eigenvalues for composite membranes. *Commun. Math. Phys.* **214** (2000) 315–337.

[12] W. Chen, C.-S. Chou and C.-Y. Kao, Minimizing eigenvalues for inhomogeneous rods and plates. *J. Sci. Comput.* **69** (2016) 983–1013.

[13] M. Cicalese and C. Trombetti, Asymptotic behaviour of solutions to p-Laplacian equation. *Asymptotic Anal.* **35** (2003) 27–40.

[14] S. Cox and R. Lipton, Extremal eigenvalue problems for two-phase conductors. *Arch. Ratl. Mech. Anal.* **136** (1996) 101–118.

[15] M.G. Crandall and P.-L. Lions, Viscosity solutions of Hamilton-Jacobi equations. *Trans. Am. Math. Soc.* **277** (1983) 1–42.

[16] F. Cuccu, B. Emamizadeh and G. Porru, Nonlinear elastic membranes involving the-Laplacian operator. *Electr. J. Differ. Equ.* **2006** (2006) 49.

[17] F. Cuccu, K. Jha, G. Porru and N. Kathmandu, Optimization problems for some functionals related to solutions of PDE'S. *Int. J. Pure Appl. Math.* **2** (2002) 399–410.

[18] B. Emamizadeh and Y. Liu, Constrained and unconstrained rearrangement minimization problems related to the p-Laplace operator. *Israel J. Math.* **206** (2015) 281–298.

[19] B. Emamizadeh and M. Marras, Rearrangement optimization problems with free boundary. *Numer. Funct. Anal. Optim.* **35** (2014) 404–422.

[20] D. Gilbarg and N.S. Trudinger, Elliptic partial differential equations of second order. Springer (2015).

[21] M. Guedda and L. Véron, Quasilinear elliptic equations involving critical Sobolev exponents. *Nonlinear Anal.: Theory, Methods & Appl.* **13** (1989) 879–902.

[22] W. Han and K.E. Atkinson, Theoretical Numerical Analysis: A Functional Analysis Framework. Springer (2009).

[23] A. Henrot, Extremum problems for eigenvalues of elliptic operators. Springer Science & Business Media (2006).

[24] D. Kang, P. Choi and C.-Y. Kao, Minimization of the first nonzero eigenvalue problem for two-phase conductors with Neumann boundary conditions. *SIAM J. Appl. Math.* **80** (2020) 1607–1628.

[25] D. Kang and C.-Y. Kao, Minimization of inhomogeneous biharmonic eigenvalue problems. *Appl. Math. Model.* **51** (2017) 587–604.

[26] C.-Y. Kao, Y. Lou and E. Yanagida, Principal eigenvalue for an elliptic problem with indefinite weight on cylindrical domains. *Math. Biosci. Eng.* **5** (2008) 315.

[27] C.-Y. Kao and S.A. Mohammadi, Extremal rearrangement problems involving Poisson's equation with Robin boundary conditions. *J. Sci. Comput.* **86** (2021) 1–28.

[28] C.-Y. Kao, S.A. Mohammadi and B. Osting, Linear convergence of a rearrangement method for the one-dimensional Poisson equation. *J. Sci. Comput.* **86** (2021) 1–18.

[29] C.-Y. Kao, S. Osher and Y.-H. Tsai, Fast sweeping methods for static Hamilton–Jacobi equations. *SIAM J Numer. Anal.* **42** (2005) 2612–2632.

[30] C.-Y. Kao and B. Osting, Extremal spectral gaps for periodic Schrödinger operators. *ESAIM: COCV* **25** (2019) 40.

[31] C.-Y. Kao and S. Su, Efficient rearrangement algorithms for shape optimization on elliptic eigenvalue problems. *J. Sci. Comput.* **54** (2013) 492–512.

[32] B. Kawohl, On a family of torsional creep problems. *J. Reine Angew. Math.* **410** (1990) 1–22.

[33] B. Kawohl and F. Schuricht, Dirichlet problems for the 1-Laplace operator, including the eigenvalue problem. *Commun. Contemp. Math.* **9** (2007) 515–543.

[34] G. Keady and A. McNabb, The elastic torsion problem: solutions in convex domains. *NZ J. Math.* **22** (1993) 43–64.

[35] G.M. Lieberman, Boundary regularity for solutions of degenerate elliptic equations. *Nonlinear Anal.: Theory, Methods Appl.* **12** (1988) 1203–1219.

[36] Y. Liu and B. Emamizadeh, Rearrangement minimization problems with indefinite external forces. *Nonlinear Anal.: Theory, Methods Appl.* **145** (2016) 162–175.

[37] Y. Liu and B. Emamizadeh, Converse symmetry and intermediate energy values in rearrangement optimization problems. *SIAM J. Control Optim.* **55** (2017) 2088–2107.
[38] M. Marras, Optimization in problems involving the-Laplacian. *Electr. J. Differ. Equ.* **2010** (2010) 2.
[39] A. Mercaldo, S.S. de León and C. Trombetti, On the behaviour of the solutions to p-Laplacian equations as p goes to 1. *Publicacions Mat.* (2008) 377–411.
[40] S.A. Mohammad, F. Bozorgnia and H. Voss, Optimal shape design for the p-Laplacian eigenvalue problem. *J. Sci. Comput.*, **78** (2019) 1231–1249.
[41] S.A. Mohammadi, Extremal energies of Laplacian operator: Different configurations for steady vortices, *J. Math. Anal. Appl.* **448** (2017) 140–155.
[42] A. Mohammadi and F. Bahrami, A nonlinear eigenvalue problem arising in a nanostructured quantum dot. *Commun. Nonlinear Sci. Numer. Simul.* **19** (2014) 3053–3062.
[43] S.A. Mohammadi and H. Voss, A minimization problem for an elliptic eigenvalue problem with nonlinear dependence on the eigenparameter. *Nonlinear Anal.: Real World Appl.* **31** (2016) 119–131.
[44] A. Mohammadi and M. Yousefnezhad, Optimal ground state energy of two-phase conductors. *Electr. J. Differ. Equ.* **2014** (2014) 1–8.
[45] P.-O. Persson and G. Strang, A simple mesh generator in MATLAB. *SIAM Rev.* **46** (2004) 329–345.
[46] G. Pólya and G. Szegö, Isoperimetric Inequalities in Mathematical Physics. (AM-27), Vol. 27. Princeton University Press (1951).
[47] S. Salsa, Vol. 99 of Partial differential equations in action: from modelling to theory. Springer (2016).
[48] J.A. Sethian, Fast marching methods. *SIAM Rev.* **41** (1999) 199–235.
[49] B. Straughan, A note on convection with nonlinear heat flux. *Ricerche di matematica* **56** (2007) 229–239.
[50] P. Tolksdorf, Regularity for a more general class of quasilinear elliptic equations. *J. Differ. Equ.* **51** (1984) 126–150.
[51] N.S. Trudinger, On Harnack type inequalities and their application to quasilinear elliptic equations. *Commun. Pure Appl. Math.* **20** (1967) 721–747.
[52] H. Zhao, A fast sweeping method for Eikonal equations. *Math. Comput.* **74** (2005) 603–627.